

The oxytocin/vasopressin-like peptide inotocin regulates cuticular hydrocarbon synthesis and water balancing in ants

Akiko Koto¹, Naoto Motoyama², Hiroki Tahara², Sean McGregor³, Minoru Moriyama⁴, Takayoshi Okabe⁵, Masayuki Miura⁵, Laurent Keller³

¹National Institute of Advanced Industrial Science and Technology, ²Department of Genetics, Graduate School of Pharmaceutical Sciences, The University of Tokyo, ³University of Lausanne, ⁴National Institute of Advanced industrial Science and Technology (AIST), ⁵The University of Tokyo

Submitted to Proceedings of the National Academy of Sciences of the United States of America

Oxytocin/vasopressin-like peptides are important regulators of physiology and social behaviour in vertebrates. However, the function of inotocin, the homologous peptide in arthropods, remains largely unknown. Here we show that the level of expression of *inotocin* and *inotocin receptor* are correlated with task allocation in the ant *Camponotus fellah*. Both genes are up-regulated when workers age and switch task from nursing to foraging. *in situ* hybridisation revealed that *inotocin receptor* is specifically expressed in oenocytes which are specialised cells synthesising cuticular hydrocarbons which function as desiccation barriers in insects and for social recognition in ants. dsRNA injection targeting *inotocin receptor*, together with pharmacological treatments using three newly-identified antagonists blocking inotocin signalling, revealed that inotocin signalling regulates the expression of *cytochrome P450 4G1 (CYP4G1)* and the synthesis of cuticular hydrocarbons, which play an important role in desiccation resistance once workers initiate foraging.

Social insect | oxytocin/vasopressin-like peptide | division of labour | behaviour tracking | cuticular hydrocarbon

Introduction

In humans and mammals, the neuropeptide hormones oxytocin and vasopressin are involved in a number of physiological processes and are increasingly implicated in a variety of social behaviours. In particular, oxytocin signalling regulates uterine contraction, lactation and energy metabolism, and has been demonstrated to increase levels of parental care, pair bonding and cooperation (1-4). Vasopressin is important for water balancing via the control of anti-diuresis, regulation of blood pressure, and plays a role in influencing social behaviours such as territorial defense, aggression and also pair bonding (5-8). Across vertebrates, oxytocin/vasopressin-like peptide homologues appear to have conserved physiological (9, 10) and behavioural functions (11-15).

An increasing number of genomic and transcriptomic analyses have revealed that a further homologue, inotocin, is specific to invertebrates where it is conserved across at least 100 species (16). This places the origin of the oxytocin/vasopressin-like peptide family prior to the split of the Protostomia and Deuterostomia, more than 600 million years ago (17). Studies on inotocin signalling in insects (16, 18-22) suggest a possible role in diuresis in *Tribolium castaneum* (18) and locomotor activity in ants (21). However, the molecular and cellular functions of inotocin signalling remain largely unknown. Given the important role of oxytocin/vasopressin-like peptides in regulating social behaviour in vertebrates (23-25), we conducted a study using ants as a model organism to investigate the physiological role of inotocin signalling and its potential implication in social behaviour.

Ants live in large and complex societies consisting of one or more reproductive queens and many non-reproductive workers (26). Workers exhibit division of labour with individuals per-

forming specific tasks within a colony (27-29). Individual task preference is generally correlated with age, with younger workers remaining inside the nest to nurse the developing offspring, and older workers foraging outside the nest. This age-based division of labour is often referred to as task polyethism, although individuals may also flexibly switch their role according to colony demands (30-32).

As workers transit from nursing to foraging, they experience new environmental challenges such as fluctuating temperatures and low humidity, both significant threats in terms of water loss and desiccation. Previous work on various insects showed that cuticular hydrocarbons (CHCs) on the body surface play an important role in protecting against desiccation (33-35). CHCs also play an important role in social recognition (36), especially to distinguish nestmates from non-nestmates in ants (37-39). It has been reported that workers change their CHC profiles before initiating foraging (40-43), possibly to better cope with the drier environment that they will encounter outside of the nest. However, the mechanisms regulating these changes remain largely unknown.

In this study, we first compare the expression of inotocin signalling in different castes and body parts of two ant species of the genus *Camponotus* and then use genetic and pharmacological manipulations to investigate the possible physiological function of this pathway. We found that *inotocin* and its receptor are most highly expressed in workers, particularly foragers, whereas queens and males show low expression levels. Histological analyses revealed that *inotocin receptor* is specifically expressed in

Significance

Inotocin, the oxytocin/vasopressin-like peptide is widely conserved in arthropods, however little is known about its molecular function. Here we show that, in ants, the expression levels of *inotocin* and its receptor are correlated with the age of workers and their behavior. We also demonstrate that inotocin signalling is involved in desiccation resistance by regulating the synthesis of cuticular hydrocarbons. We propose that the up-regulation of *inotocin* and its receptor as workers age and switch task from nursing to foraging is a key physiological adaptation to survive drier environments outside of the nest.

Reserved for Publication Footnotes

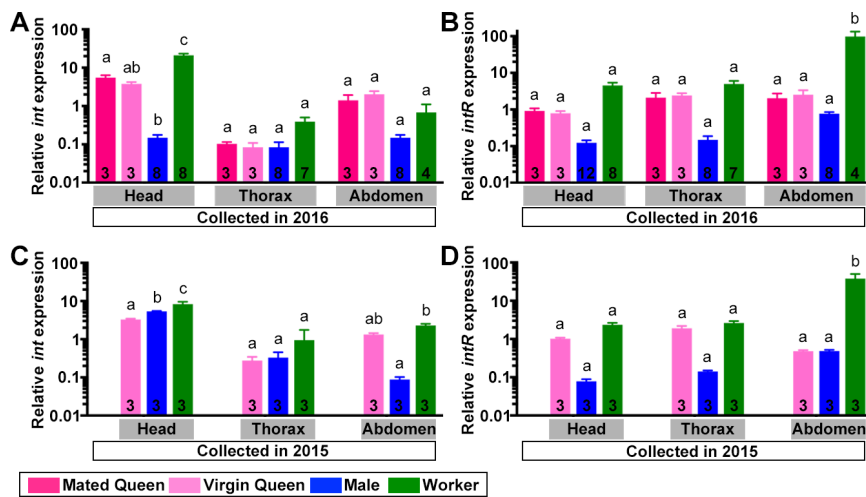


Fig. 1. Relative expression of inotocin and inotocin receptor in different castes and tissues of *Camponotus japonicus* Relative expression (mean \pm SEM) of *inotocin* (*int* in A and C) and *inotocin receptor* (*intR* in B and D) in the head, thorax and abdomen of virgin queens (pink), mated queen (red), males (blue) and workers (green). The expression of each gene was scaled by the average value in each graph. Values are therefore not comparable between graphs. Number of individuals are shown in each box. The relative expression levels of each gene were tested with two-way ANOVA. Groups differing significantly ($p < 0.05$) are marked with different letters. Samples shown in panel A and B were collected in 2016 and samples in panels C and D in 2015. We did not collect any mated queen in 2015.

the oenocytes, a type of specialised cell that produces CHCs in insects (44-46). We also show that inotocin signalling regulates the expression of CHCs via *CYP4G1*, the key enzyme for hydrocarbon synthesis (45, 46). Based on these results, we propose that inotocin signalling is a key regulator of hydrocarbon metabolism, which in turn may allow an adaptive plastic response as workers transition from the relatively safe environment of the nest to a hostile foraging environment.

Results

Expression profiles of *int/intR* in reproductive castes

To compare the expression levels of *inotocin* (*int*) and *inotocin receptor* (*intR*) among castes, we collected young virgin queens, mated queens, males, and workers of the carpenter ant *Camponotus japonicus* in 2016. There was substantial variation in levels of *int* mRNA among body parts (head, thorax and abdomen; $F_{49}=47.3, p < 0.0001$) and castes (virgin queens, mated queens, males and workers; $F_{49}=30.2, p < 0.0001$) as well as a significant interaction between body parts and castes ($F_{49}=31.4, p < 0.0001$, Fig. 1A and SI Appendix, Table S1). In the head, the level of expression was high in workers, intermediate in the two types of queens and low in males. In the thorax, the levels of expression were very low in each of the four castes while in the abdomen, the levels of expression were intermediate with no significant differences among castes.

The expression of the *intR* was significantly different between body parts ($F_{53}=11, p=0.0001$) and castes ($F_{53}=18.3, p < 0.0001$). There was also a significant interaction between body parts and castes ($F_{53}=12.2, p < 0.0001$, Fig. 1B and SI Appendix, Table S1). In the head and thorax, *intR* expression was very high in workers, intermediate in queens and very low in males. In the abdomen, the level of expression was significantly higher in workers than males and the two types of queens. Similar results were obtained in *C. japonicus* samples collected in 2015 (Fig. 1C and 1D, and SI Appendix, Table S1).

To investigate the role of inotocin signalling on social behaviour, we conducted a detailed analysis of the expression of *int* and *intR* in workers. Because it is difficult to control for worker age and precisely determine worker task in the field, we used *Camponotus fellah* workers from colonies established from founding queens collected in 2003 and 2007 throughout all of the following experiments. We firstly confirmed that the expression profiles in reproductive castes of *C. fellah* are similar with those of *C. japonicus* (SI Appendix, Fig. S1 and Table S1), with the difference that the expression of *int* mRNA is higher in the heads of males than queens and workers.

Correlation between *int/intR* expression and task allocation in workers

To determine the approximate age of each worker in the laboratory-reared *C. fellah* colonies, we colour-marked newly-enclosed workers every month. Task allocation was defined by the spatial location of the ants in the rearing box, 'nurses' being workers collected in the nest and 'foragers' those in the foraging arena (Fig. 2A). There was a significant association between age and foraging propensity ($\chi^2=255.2, p < 0.0001$, Fig. 2B). Individuals started foraging after they were 4-months old with a significant increase in the proportion of foraging with increased age (Fig. 2B and SI Appendix, Fig. S2A-C).

Given that *int* is predominantly expressed in the heads (Fig. 1A, 1C and SI Appendix, Fig. S1A), we compared the expression profiles of *int* in heads of nurses and foragers of different age classes. *int* expression was significantly associated with age ($F_{184}=3.6, p=0.0023$) and task ($F_{186}=4.4, p=0.037$; age x task interaction: $F_{185}=0.056, p=0.94$). The level of expression of *int* was lowest in young nurses and highest in old foragers (Fig. 2C). The level of *int* expression was also significantly higher in foragers than nurses within one of the three age classes containing both types of workers (5-month old individuals: $F_{30}=4.8, p=0.037$, SI Appendix, Table S2). Given that *intR* is predominantly expressed in the abdomen (Fig. 1B, 1D and SI Appendix, Fig. S1B), we compared the expression profiles of *intR* in the abdomens of nurses and foragers of different age classes. Similar to *int* in the head, there was a significant effect of age on *intR* expression ($F_{178}=26.5, p < 0.0001$, Fig. 2D) and an interaction effect between age and task ($F_{178}=4.2, p=0.017$) but *intR* expression was not significantly associated with task ($F_{178}=0.37, p=0.54$). There was, however, a significant difference in *intR* expression between nurses and foragers within two of the three age classes containing both types of workers (5-month old: $F_{34}=10.8, p=0.0024$, and 6-month old: $F_{31}=5.3, p=0.028$, SI Appendix, Table S2). These results suggest that *int* and *intR* expression are associated not only with age, but also with the task performed by workers.

To further investigate the role of *int* and *intR* on division of labour and to control for age-dependent effects, we set up nine groups each containing 10 4-month old nurses and monitored their behaviour as division of labour was re-organised with those that remained as nurses, and others who started foraging. We measured activity level, time in the food region and time in the nest (Fig. 2E and SI Appendix, Fig. S2D) with an automated video tracking system (47) during six days. The level of *int* expression in the whole body was positively correlated with the overall level of activity ($F_{71}=48.9, p < 0.0001$, Fig. 2G) but not the amount of

273
274
275
276
277
278
279
280
281
282
283
284
285
286
287
288
289
290
291
292
293
294
295
296
297
298
299
300
301
302
303
304
305
306
307
308
309
310
311
312
313
314
315
316
317
318
319
320
321
322
323
324
325
326
327
328
329
330
331
332
333
334
335
336
337
338
339
340

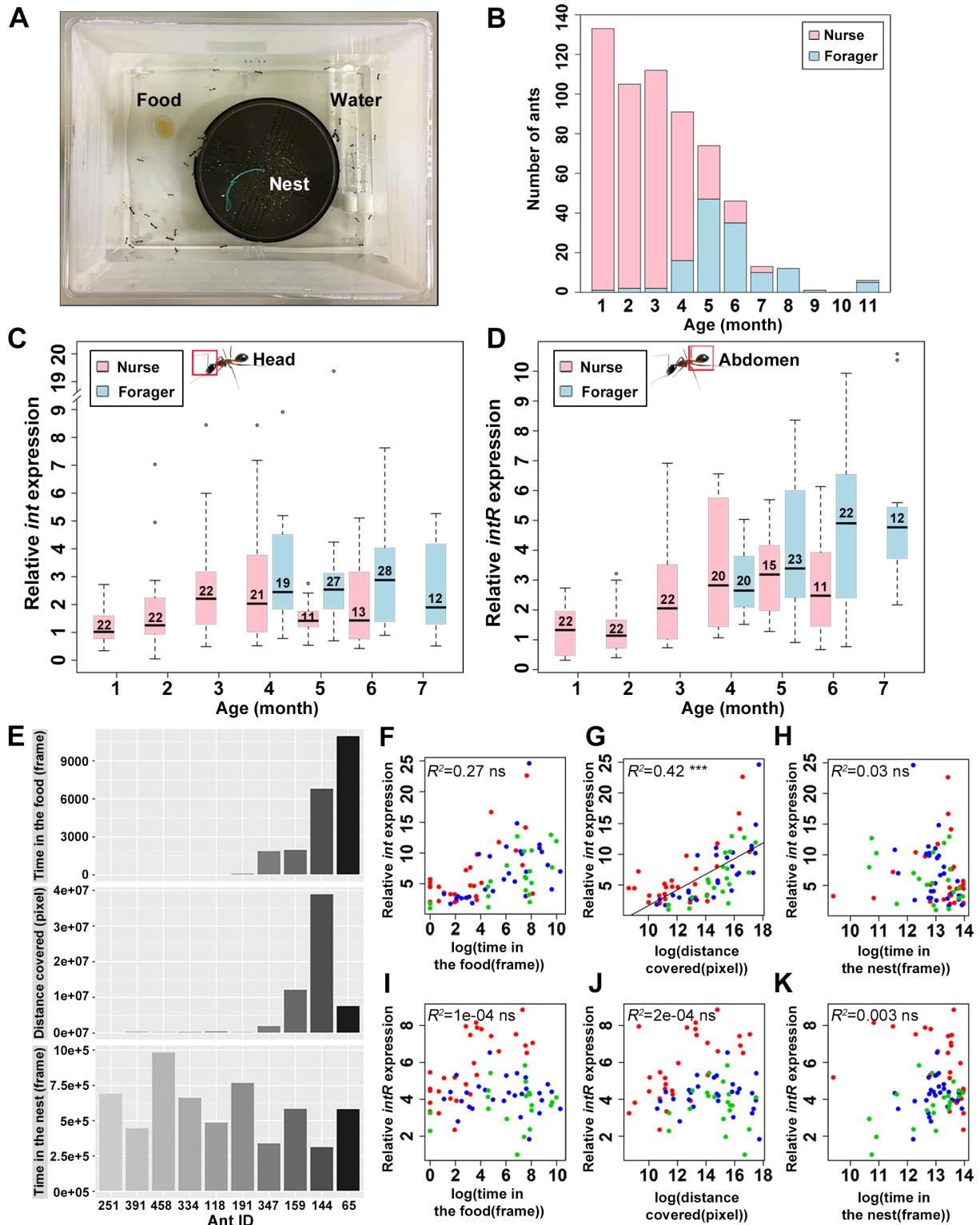


Fig. 2. Correlation between the expression of inotocin signalling and task allocation (A) Setup of the *Camponotus fellah* colonies. (B) Age-dependent division of labour in one representative colony. Nurses are shown in pink, and foragers in the light blue. (C and D) Box-plots of the relative expression levels of *int* in the head (C) and *intR* in the abdomen (D) for each age class. Number of individuals is shown in each box. (E) The time spent in the food region and in the nest and distance moved was quantified over six days in the tracking system for one representative box. (F-H) Relationship between the behavioural parameters and *int* expression. (I-K) Relationship between the behavioural parameters and *intR* expression. Different colours indicate the colony of origin of workers. R^2 and p -values are shown on the top left of the graphs. The correlation between the expression of *int* or *intR* and behavioural parameters were tested with GLMM. ns $p>0.05$; *** $p<0.001$.

time spent in the food region ($F_{71} = 2.3$, $p = 0.13$, Fig. 2F) nor time spent in the nest ($F_{71} = 0.25$, $p = 0.62$, Fig. 2H). The level

of expression of *intR* was not significantly correlated with any of these three behavioural measures (time in the food region:

341
342
343
344
345
346
347
348
349
350
351
352
353
354
355
356
357
358
359
360
361
362
363
364
365
366
367
368
369
370
371
372
373
374
375
376
377
378
379
380
381
382
383
384
385
386
387
388
389
390
391
392
393
394
395
396
397
398
399
400
401
402
403
404
405
406
407
408

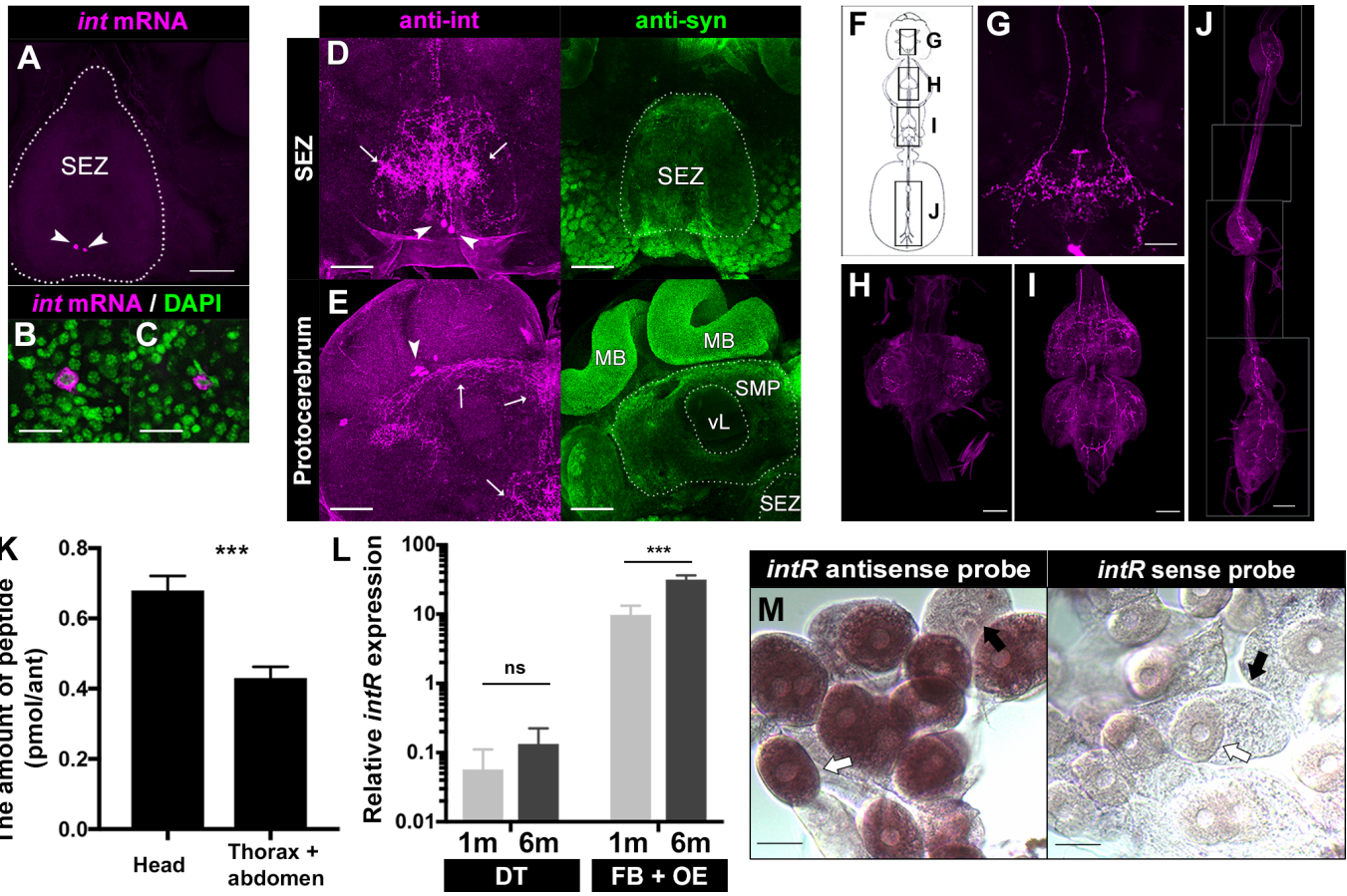


Fig. 3. The expression of *inotocin* in neural tissues and *inotocin* receptor in the fat body plus oenocytes (A) Fluorescent *in situ* hybridisation using specific *int* antisense probe (shown in magenta). Arrowheads indicate the pair of neurons labelled with *int* mRNA in subesophageal zone (SEZ, outlined with white dotted line). (B and C) Magnified image of each *int* mRNA positive neuron (shown in magenta in A) with stained nucleus using DAPI (shown in green). (D and E) Immunohistochemistry for anti-*int* antibody (shown in magenta) and anti-synapsin antibody (shown in green) in SEZ (D) and protocerebrum (E). Arrowheads indicate cytoplasmic expression of anti-*int* immunoreactivity. Arrows indicate the neurons positive with anti-*int* antibody in SEZ (D) and protocerebrum (E), in which brain compartments are labelled as mushroom body (MB), medial superior protocerebrum (SMP), and vertical lobe (vL). (F) Schematic presentation from central to peripheral nervous system in workers. (G-J) One pair of neurons labelled with anti-*int* antibody from subesophageal zone to ventral nerve cord (G), the prothoracic (H), mesothoracic and metathoracic (I), and abdominal ganglia (J). (K) Distribution of endogenous inotocin peptide tested with unpaired two-tailed *t*-test. *** $p < 0.001$. (L) qRT-PCR for the *intR* in the digestive tract (DT) and fat body plus oenocytes (FB+OE). The expression of *intR* mRNA was tested with GLMM with Benjamini-Hochberg *post-hoc* test. ns $p > 0.05$; *** $p < 0.001$. (M) *in situ* hybridisation using *intR* antisense probe (upper panel) and sense probe (bottom panel) in the dissected fat body plus oenocytes. Oenocytes are indicated with open arrows and trophocytes (the lipid storing cells of the fat body) with filled arrows. Scale bars, 100 μ m (A, D, E, G-J), 20 μ m (B, C, and M).

$F_{70}=0.14, p=0.71$, Fig. 2I; distance covered: $F_{70} = 1.24, p=0.27$, Fig. 2J; time in the nest: $F_{70} = 3.79, p=0.06$, Fig. 2K). A similar experiment conducted with younger (1 to 2-month old) workers (SI Appendix, Fig. S3) revealed a similar pattern for *int*, but the level of expression of *intR* was also significantly associated with the overall level of activity (*int*; $F_{43}=12.3, p=0.001$, SI Appendix, Fig. S3F, *intR*; $F_{44}=21.2, p < 0.0001$, SI Appendix, Fig. S3I). These results further support the view that the expression levels of *int* and *intR* are both associated with the age and the behaviour of workers.

Cellular localisation of *int* and *intR* in workers

To better understand the function of inotocin signalling, we next looked for cellular localisation of *int* in the head and *intR* in the abdomen of workers. Fluorescent *in situ* hybridisation with an *int* gene probe revealed highly specific expression of *int* mRNA in one pair of neurons of the subesophageal zone (indicated with arrowheads in Fig. 3A and magnified in Fig. 3B and 3C). This expression pattern is similar to that of anti-vasopressin antibody staining in locusts (18) and ant *Lasius neglectus* (21). To further clarify the localisation of inotocin proprotein we created an antibody against the inotocin proprotein (anti-*int*) targeting the C-

terminus region of the inotocin proprotein (SI Appendix, Fig. S4A-C). To examine whether the expression of *int* mRNA and its proprotein were in the same cells of the subesophageal zone, we performed sequential staining with immunohistochemistry and fluorescent *in situ* hybridisation which confirmed that the two neurons of the subesophageal zone expressing *int* mRNA were also labelled with anti-*int* antibody (shown in the upper panel in SI Appendix, Fig. S4D). By contrast, no signal was found when performing a negative control immunostaining with an anti-*int* antibody pre-absorbed with the antigen peptide (bottom panel in SI Appendix, Fig. S4D), consistent with specificity of the immunoreactive signals labelled with anti-*int* antibody.

In addition to a pair of neurons in subesophageal zone (indicated with arrowheads in Fig. 3D), we identified a cluster of neurons labelled with anti-*int* antibody in protocerebrum (Fig. 3E). They spread from the subesophageal zone to the lateralis of medial superior protocerebrum (indicated with arrows in Fig. 3D and 3E). Cytoplasmic immunoreactivity of anti-*int* antibody on the lateralis of protocerebrum (indicated with arrowheads in Fig. 3E) was very similar to the neurosecretory neurons expressing

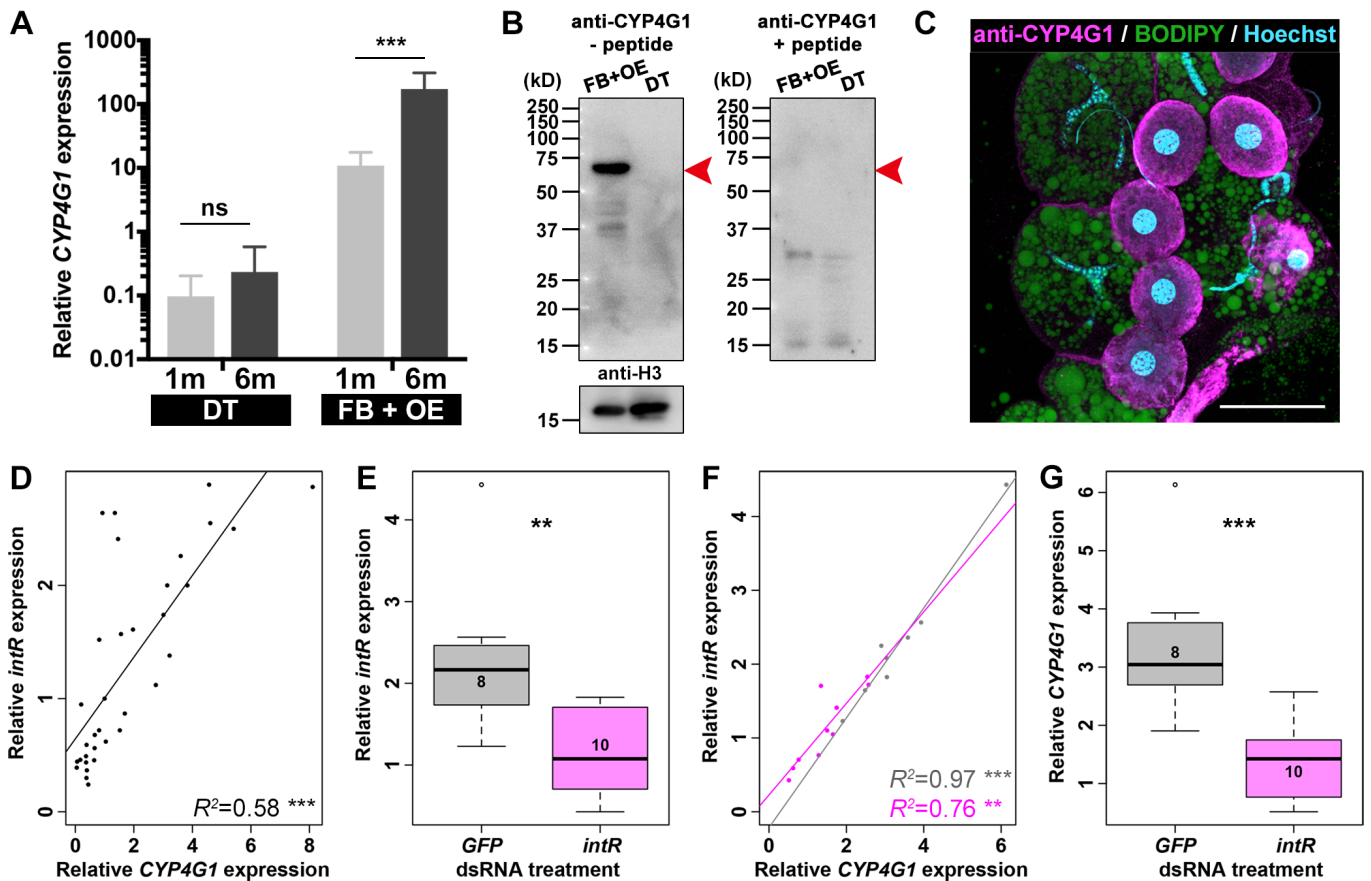


Fig. 4. Expression of CYP4G1 correlating with that of inotocin receptor (A) qRT-PCR data for *CYP4G1* expression in the digestive tract (DT) and fat body plus oenocytes (FB+OE) for 1- and 6-month old individuals. $**p < 0.01$; $***p < 0.001$ (GLMM with Benjamini-Hochberg *post-hoc* tests). (B) The CYP4G1 protein is expressed in the fat body plus oenocytes (FB+OE) but not in the digestive tract (DT). The band at 63kD (shown with red arrowhead in the left panel) was not detected with the anti-CYP4G1 antibody after the absorption with its antigen peptide (right panel). (C) The CYP4G1 protein (magenta) is specifically present in the oenocytes (round-shaped nucleus stained with Hoechst, light blue), but not in the trophocytes (irregular shaped nucleus and lipid droplets labelled with BODIPY, green). Scale bar, 50 μ m. (D) Correlation between the expression of *CYP4G1* and *intR* in the abdomen. R^2 and p -values are shown on the bottom right of the graph. $***p < 0.001$. (E) Feeding of dsRNA targeting *intR* leads to a significant decrease in the level of expression of *intR* (magenta, unpaired two-tailed t -test, $**p < 0.01$) compared to feeding of dsRNA targeting *GFP* (grey). Number of individuals is shown in each box. (F) Relationship between the expression levels of *intR* and *CYP4G1* in the treatment with dsRNA targeting *GFP* (grey) and *intR* (magenta). R^2 and p -values for each treatment are shown on the bottom right of the graph. (G) *CYP4G1* expression is significantly down-regulated with feeding dsRNA targeting *intR* (magenta, unpaired two-tailed t -test) compared to feeding of dsRNA targeting *GFP* (grey). Number of individuals is shown in each box.

PERIOD in honeybees (48), suggesting that these immunoreactive neurons may also have a neurosecretory role.

Additional immunohistochemistry with anti-int antibody revealed a pair of descending axons coming from the cell bodies in subesophageal zone, which are spanning the length of the ventral nerve cord (Fig. 3F and 3G) and extending through the prothoracic (Fig. 3H), mesothoracic, metathoracic (Fig. 3I) and abdominal ganglia (Fig. 3J).

We next examined the expression profile of endogenous inotocin peptide between the head, thorax and abdomen of 6-month old foragers. LC-MS/MS revealed the distribution of inotocin peptide between tissues, with the highest level of inotocin peptide in the head ($t_{10} = 4.8$, $p = 0.0007$, Fig. 3K). This result is consistent with the highest expression of *int* mRNA in the head, suggesting that the inotocin peptide is mainly expressed in the central nervous system, as is the case with oxytocin and vasopressin in mammals. In addition, the distribution of inotocin peptide in the thorax and abdomen suggests that inotocin peptide could activate its receptor which is highly expressed in the abdomen (Fig. 1B, 1D, and 2D).

Next, we examined in which specific tissues of the abdomen *intR* was expressed. We focused on the digestive tract, fat body and oenocytes which are interspersed within the fat body in

ants (49, 50). Because it is technically very difficult to separate oenocytes from the fat body we extracted RNA from the fat body plus oenocytes. We found that *intR* mRNA was expressed at significantly greater levels in the fat body plus oenocytes than in the digestive tract (age effect, $F_{30} = 148$, $p < 0.0001$, tissue effect, $F_{30} = 525$, $p < 0.0001$, tissue x age interaction, $F_{30} = 145$, $p < 0.0001$, Fig. 3L), implicating the fat body or oenocytes as a likely tissue expressing *intR* in the abdomen. In addition, there was a strong age effect ($p < 0.0001$, Fig. 3L) with 6-month old workers expressing significantly higher levels of *intR* in the fat body plus oenocytes than 1-month old workers. This result is consistent with expression data from the whole abdomen (Fig. 2D).

To determine the source of *intR* expression at the cellular level we conducted *in situ* hybridisation. These analyses revealed specific expression in the oenocytes which can be recognised by their round-shaped nucleus (see open arrows, upper panel Fig. 3M). By contrast there was no signal in the trophocytes which are the main cells of the fat body and are recognisable by their irregular nucleus (see filled arrows, upper panel Fig. 3M). Taken together these data indicate that the inotocin protein is expressed in the central and peripheral nervous systems and then transferred through to the abdomen where it likely activates inotocin receptor sites specifically expressed in the oenocytes.

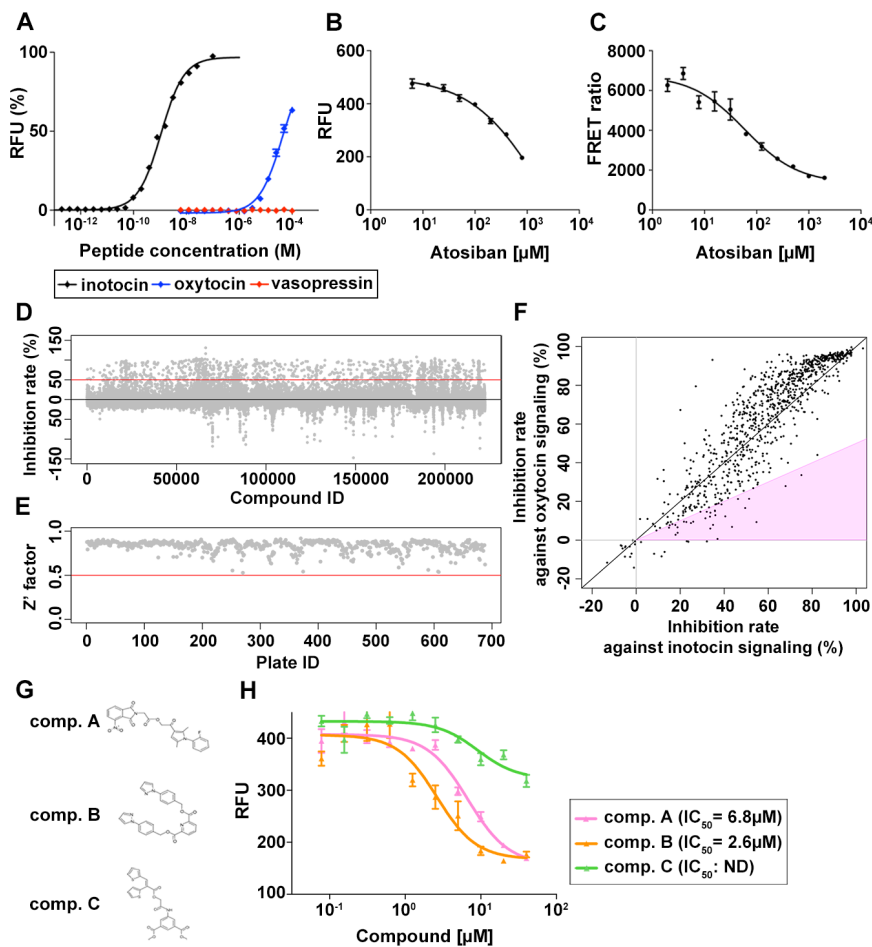


Fig. 5. Chemical screening to identify the inhibitor against inotocin signalling (A) Relative fluorescent intensity (RFU) of Fluo-4 probe in response to inotocin, oxytocin and vasopressin in CHO cells expressing inotocin receptor. Inotocin receptor is activated by inotocin (black line, $EC_{50}=1.1\text{ nM}$), oxytocin (blue line, $EC_{50}=41.6\text{ }\mu\text{M}$), but not by vasopressin (red line). (B) Atosiban blocks the activation of inotocin signalling ($IC_{50}=599\text{ }\mu\text{M}$). 5nM inotocin was used as an approximate EC_{80} concentration. Data represents the mean \pm SEM (n=3). (C) Competition curve of specific binding of 10nM labelled-inotocin ligand with increasing concentrations of atosiban (1.95 μM -2mM) measured by TR-FRET. Data represent the mean \pm SEM of a representative experiment (n=3). TR-FRET ratio=(665 nm acceptor signal/620 nm donor signal) \times 10,000. (D) Scatter plot showing the inhibition rate of each compound in the 1st screening. The red line indicates a 50% inhibition. (E) Scatter plot showing the Z' factor for each plate in the 1st screening. All Z' factor in each plate are more than 0.5 indicated by the red line. (F) Inhibition rate against inotocin and oxytocin signalling are plotted for each of the 902 compounds showing >50% inhibition rate in the 1st screening. Compounds showing <50% inhibition rate for inotocin than oxytocin are in the pink shadowed region. (G) Structure of three compounds A, B and C. (H) Dose-dependent inhibition against inotocin signalling of comp. A ($IC_{50}=6.8\text{ }\mu\text{M}$, pink line), comp. B ($IC_{50}=2.6\text{ }\mu\text{M}$, orange line), and comp. C (IC_{50} : no data, green line). Data represent the mean \pm SEM of a representative experiment (n=4). Relative fluorescent unit (RFU) indicates the activation of inotocin receptor calculated from Fluo-4 intensity.

Correlation between *intR* and *CYP4G1* expression

Given that *intR* is expressed in oenocytes, we investigated the relationship between inotocin signalling and the CHC synthesis pathway to which the cells primary function is linked. We firstly focused on the *CYP4G1* gene, which is an aldehyde oxidative decarbonylase P450. This gene is highly conserved in insects and is known to be expressed in the oenocytes (44-46), where it regulates the final step of CHC synthesis by converting aldehyde to hydrocarbons (45). We found higher expression of *CYP4G1* in the fat body plus oenocytes than in the digestive tract (age effect, $F_{30}=12.4$, $p=0.0014$, tissue effect, $F_{30}=220$, $p<0.0001$, tissue \times age interaction, $F_{30}=9.8$, $p=0.0038$, Fig. 4A). The expression of *CYP4G1* was higher in the fat body plus oenocytes of 6-month old than 1-month old workers ($p<0.0001$, Fig. 4A). A similar pattern was found by using a specific antibody against CYP4G1 protein, with CYP4G1 expressed in the fat body plus oenocytes but not in the digestive tract (Fig. 4B). Immunohistochemistry with this antibody further revealed that the CYP4G1 protein is specifically expressed in the oenocytes but not in the trophocytes (Fig. 4C). In addition to the similarity between the histological expression of CYP4G1 (Fig. 4C) and *intR* (Fig. 3M), the expression of *CYP4G1* mRNA is up-regulated in an age-dependent manner both in the head (SI Appendix, Fig. S5A) and abdomen (SI Appendix, Fig. S5B), and there was also a positive correlation between the expression of these two genes in the abdomen ($R^2=0.58$, $t_{32}=6.6$, $p<0.0001$, Fig. 4D).

To study the relationship between inotocin signalling and *CYP4G1* expression, we performed a RNA interference assay by feeding 5-month old workers with dsRNA targeting *intR* with the

previously described protocol (51). Workers fed with dsRNA of *intR* showed a lower level of expression of *intR* in the abdomen than control ants ($t_{16}=3.3$, $p=0.0044$, Fig. 4E). Moreover, the expression of the *intR* was significantly correlated with the expression of *CYP4G1* in both ants treated with dsRNA of *intR* ($R^2=0.76$, $t_8=5.04$, $p=0.001$, Fig. 4F) and control ants treated with dsRNA of *GFP* ($R^2=0.97$, $t_6=14.36$, $p<0.0001$, Fig. 4F), resulting in the down-regulation of *CYP4G1* expression in the dsRNA of *intR* treated ants ($t_{16}=4.06$, $p=0.0009$, Fig. 4G).

Identification of antagonists that block inotocin signalling

We next developed a pharmacological protocol to inhibit inotocin signalling. We established a Chinese hamster ovarian (CHO) cell line which stably expressed the inotocin receptor and monitored the activation of the receptor against inotocin peptide by measuring the increase in cytosolic calcium concentration with the fluorescent calcium probe Fluo-4. We confirmed that the inotocin receptor is activated by the synthesised inotocin peptide in a dose-dependent manner ($EC_{50}=1.09\text{ nM}$, Fig. 5A) as previously described (21, 22, 52). We also showed that the inotocin receptor is activated by oxytocin ($EC_{50}=41.6\text{ }\mu\text{M}$, Fig. 5A) but not vasopressin (Fig. 5A), suggesting the possibility that oxytocin antagonists may also inhibit inotocin signalling. To test this, we used atosiban, an oxytocin analogue with the modification of amino acids at 1, 2, 4 and 8, which is medically used for the treatment of preterm labour (53). The activation of the inotocin receptor by inotocin was inhibited by atosiban in a dose-dependent manner ($-IC_{50}=599\text{ }\mu\text{M}$, Fig. 5B), although this effect was weaker than against oxytocin signalling ($IC_{50}=0.65\text{ }\mu\text{M}$, SI Appendix, Fig. S6) (54, 55). To examine whether atosiban

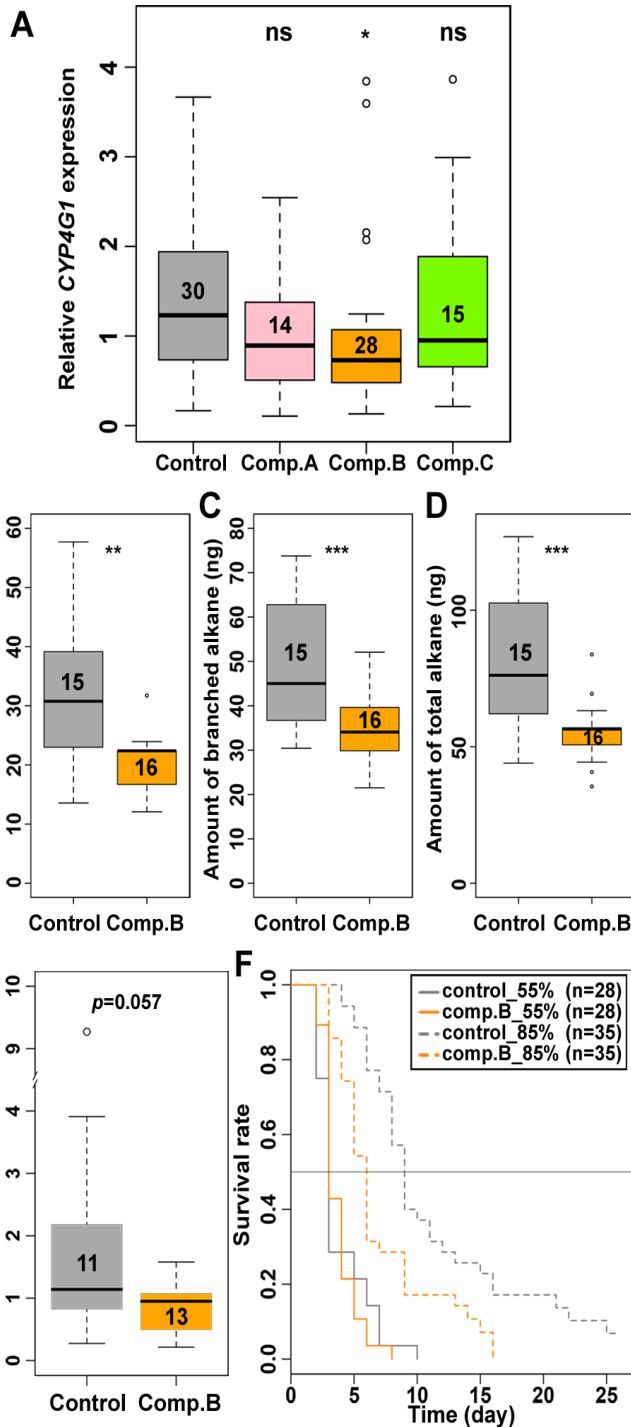


Fig. 6. Relationship between inotocin signalling, hydrocarbon synthesis and desiccation resistance(A) *CYP4G1* expression (qRT-PCR) for comp. A-treated, comp. B-treated, comp. C-treated and control 4-month old workers. ns $p > 0.05$; * $p < 0.05$ (GLMM with Dunnett *post-hoc* tests). (B-D) The quantities of normal (B), branched (C) and total alkanes (D) in comp. B-treated and control >5-month old workers. (E) qRT-PCR for *CYP4G1* in comp. B-fed and control 4-month old workers. Number of individuals is shown in each box. The data were analysed with GLMMs. ** $p < 0.01$; *** $p < 0.001$. (F) Survival curves for control (grey) and comp. B-treated (orange) ants in 55% RH (solid line) or 85% RH (dashed line). Sample sizes are as follows; $n = 28$ for ctrl.55% and comp. B.55%, and $n = 35$ for ctrl.85% and comp. B.85%.

prevents binding of inotocin to inotocin receptor, as is the case with oxytocin (56), we performed a time-resolved fluorescence

resonance energy transfer (TR-FRET) assay to measure the binding efficiency between inotocin and inotocin receptor. Atosiban treatment resulted in a dose-dependent decrease in the FRET ratio ($IC_{50} = 58.8 \mu M$, Fig. 5C), indicating that it directly inhibits binding between inotocin and its receptor, thereby functioning as an antagonist of inotocin signalling. Because the inhibition effect of atosiban against inotocin signalling was not as strong as against oxytocin signalling, we performed a high throughput chemical screening to identify novel chemical compounds acting as antagonists to inotocin signalling.

In the first screening with 224,400 chemical compounds library, we obtained 902 compounds whose inhibition rate against inotocin signalling was higher than 50% (Fig. 5D). The Z' value (a parameter assessing the robustness of an assay for high throughput screening) was more than 0.5 in all assay plates, indicating that the system was adequately optimised for the screening (Fig. 5E). Here it is expected that these candidate chemicals contain nonspecific compounds blocking not only inotocin signalling but also other signalling pathways, for example by targeting factors common with the G protein coupled-receptor (GPCR) pathway. To exclude such non-specific inhibition, we performed a second screening in which we examined the inhibitory effects of each compound against both inotocin and oxytocin signalling (Fig. 5F). If the effector site of these candidates is inotocin receptor itself, the inhibition rate against oxytocin signalling should be weaker than against inotocin signalling. Twenty-three compounds showed higher inhibition rate against inotocin signalling than oxytocin signalling (pink-shaded region in Fig. 5F). Among these 23 candidates, three chemicals (named comp. A, comp. B, or comp. C in Fig. 5G) showed an inhibition rate that was less than half on oxytocin signalling than on inotocin signalling even in tests with the higher dosage (20 μM) of each compound. These three chemicals also showed a dose-dependent inhibition against inotocin signalling (Fig. 5H) and were therefore selected for studying the role of inotocin signalling on CHC synthesis.

Regulation of cuticular hydrocarbon synthesis via inotocin signalling

To study the effect of antagonists *in vivo*, we injected compounds A, B and C into 4-month old workers and examined the expression of *CYP4G1* with qRT-PCR. If these compounds inhibit inotocin signalling, the injection of each compound should, similar to the *intR* dsRNA treatment, lead to a down-regulation of *CYP4G1* expression. Consistent with this reasoning, *CYP4G1* expression was lower in workers injected with compound A, B and C, although the difference was only significant for compound B ($p = 0.042$, Fig. 6A). In addition, we found that *CYP4G1* expression was also significantly down-regulated by atosiban (1 mM: $p = 0.026$, 2 mM: $p = 0.0002$, SI Appendix, Fig. S7A). These results, together with those of the dsRNA treatment, indicate that inotocin signalling positively regulates *CYP4G1* expression.

We next examined whether down-regulation of *CYP4G1* expression has a quantitative effect on the expression of CHCs by testing compound B, the antagonist that most effectively inhibited inotocin signalling *in vitro* (Fig. 5H), and significantly down-regulated the expression of *CYP4G1* (Fig. 6A). In *C. fellah*, and broadly speaking in ants, CHCs are mostly composed of long chain saturated (normal) and methyl-branched (branched) alkanes (37). We found that the quantity of normal alkanes was higher in foragers than nurses ($F_{22} = 9.4$, $p = 0.006$, SI Appendix, Fig. S8A), though neither the quantities of branched alkanes ($F_{22} = 1.1$, $p = 0.3$, SI Appendix, Fig. S8B), nor total alkanes ($F_{22} = 0.6$, $p = 0.45$, SI Appendix, Fig. S8C) was significantly different between the two types of workers. By comparing the quantity of CHCs between control and compound B-injected >5-month old workers, we found that compound B-treated ants had reduced quantities of normal alkanes ($F_{28} = 13.5$, $p = 0.001$, Fig. 6B) and branched alkanes ($F_{27} = 16.5$, $p = 0.0004$, Fig. 6C). Ac-

953 cordingly, the total quantity of alkanes was also significantly lower
954 ($F_{27}=16.7$, $p=0.0004$, Fig. 6D). Injection of 2mM atosiban also
955 led to reduced quantities of normal alkanes ($F_{40}=7.75$, $p=0.008$,
956 SI Appendix, Fig. S7B) and a tendency for reduced branched
957 alkanes ($F_{40}=3.1$, $p=0.088$, SI Appendix, Fig. S7C), with the
958 effect that the total quantity of alkanes was also significantly lower
959 ($F_{40}=6.87$, $p=0.012$, SI Appendix, Fig. S7D).

960 If down-regulation of *CYP4G1* decreases production of
961 CHCs, we predicted that ants treated with compound B should
962 have lower resistance to desiccation and survive less well in an
963 environment where water intake is restricted. To test this, we
964 compared the survivability of workers fed with 1 μ M compound
965 B (treatment) with those treated with 1% DMSO (control) when
966 given no access to water. We first confirmed that ants fed with
967 compound B had a tendency for lower expression of *CYP4G1*
968 than control ants ($F_{22}=4.03$, $p=0.057$, Fig. 6E), as previously ob-
969 served in the injection assays (Fig. 6A). To manipulate desiccation
970 rates, we placed seven workers in a box at either 55% relative
971 humidity (RH) or 85% RH. Under 55% RH both treatment and
972 control workers died rapidly and there was no difference in
973 survival ($p=0.76$), suggesting that these experimental conditions
974 were too severe for ants, regardless of treatment. Under the
975 85% RH condition both treatment and control groups survived
976 significantly longer ($p<0.0001$, Fig. 6F) and there was a significant
977 lower survival for ants treated with compound B compared to
978 control ants ($p=0.026$, Fig. 6F). This suggests that in conditions
979 where water is absent ants are capable of surviving longer with
980 intact *CYP4G1* and CHC function.

982 Discussion

983 Our study reveals that the levels of *int* and *intR* mRNA are very
984 high in workers, and positively correlated with age and foraging
985 behaviour. Moreover, when ants of the same age were placed into
986 a new artificial nest and allowed to re-establish division of labour,
987 those initiating foraging had higher levels of *int* or *intR* expression
988 than those staying within the nest, suggesting that inotocin sig-
989 nalling may be linked to the onset of foraging behaviour in ants.
990 The levels of expression of oxytocin and vasopressin is known
991 to also influence social behaviour in mammals. For example,
992 the level of social investigation is associated with the level of
993 expression of *oxytocin* and *vasopressin* mRNA in mice (57). In
994 mice, the level of expression of *vasopressin* is also correlated with
995 aggressive behaviour (58, 59) while oxytocin signalling is involved
996 with social bonding and affiliation (4, 60, 61).

998 CHCs are known to prevent desiccation in insects (33-35)
999 and recent work on flies supports the hypothesis that increased
1000 CHC production improves desiccation resistance (62). In ants,
1001 desiccation is an important challenge when workers switch task
1002 and initiate foraging. We found that *C. fellah* workers switch task
1003 when they are 4-months old. Similar results were obtained in
1004 other studies (32, 47). As workers age, they experience a drastic
1005 change in their environment as they switch from brood care and
1006 other within-nest tasks to foraging outside of the colony. Factors
1007 such as humidity and temperature can vary greatly over time and
1008 space outside the nest while they are relatively stable within the
1009 nest. Similar to findings in the ants *Pogonomyrmex barbatus* and
1010 *Formica exsecta* (40-43), we found task-associated variation in
1011 CHCs, with foragers exhibiting the highest proportion of normal
1012 alkanes. Moreover, experimental increments of temperature and
1013 decreases in humidity also triggered an increase in the proportion
1014 of normal alkanes in harvester ants (41). Given that we found
1015 that *intR* is expressed in the oenocytes, we investigated the re-
1016 lationship between inotocin signalling and the CHC synthesis
1017 pathway. We focused on the *CYP4G1* gene, which is known to
1018 be expressed in oenocytes (44-46), where it regulates the final
1019 step of CHC synthesis by converting aldehyde to hydrocarbons
1020 (45). Using immunohistochemistry, we first confirmed that the

CYP4G1 protein is specifically expressed in the oenocytes in
workers. Next, we showed a strong positive association between
the levels of expression of *intR* and *CYP4G1*, suggesting that
increased levels of *intR* expression might be associated with in-
creased level of *CYP4G1* when workers start foraging. These lines
of evidence suggest foraging ants are able to reduce the risk
of desiccation through up-regulation of the inotocin signalling
pathway, generating elevated quantities of protective CHCs.

Because variation in task allocation is associated with vari-
ation in CHCs not only in *C. fellah* (this study) but also in the
two other ants that have been investigated so far (i.e., *P. barbatus*
and *F. exsecta*, (40-43)), it would be interesting to test whether
inotocin signalling does also regulate the production of CHCs in
these species. In the ants *Lasius niger* and *Lasius neglectus*, the
level of expression of *intR* has also been shown to be higher in
the abdomen than head and thorax (21), suggesting that this gene
might also be implicated in the production of CHCs. Moreover,
as in *C. fellah*, the expression of *int* is also higher in the head of
foragers than nurses in the ant *Monomorium phararonis* (63). The
similarity in the expression profiles of *inotocin* and *inotocin recep-*
tor in the ant species that have been studied so far suggests that
inotocin signaling may, as in *C. fellah*, also function to regulate
the expression of CHCs in other ant species.

To provide functional evidence for a role of *intR* on the
level of expression of *CYP4G1* we fed 5-month old workers with
dsRNA targeting *intR*. These treated workers exhibited a lower
level of expression of both *intR* and *CYP4G1* compared to control
ants. Next, we conducted pharmacological studies to identify
new compounds acting as antagonists of the inotocin signalling
pathway. These studies identified three effective antagonist com-
pounds (named A, B and C). Injection of these antagonists led
to decreased expression of *CYP4G1*. Finally, *CYP4G1* expression
was also significantly down-regulated by atosiban, an inhibitor
of oxytocin in vertebrates (64, 65), which we showed to also
be effective in decreasing the activation of inotocin receptor
by inotocin *in vitro*. Together, these results show that inotocin
signalling positively regulates *CYP4G1* expression.

Our experiments also showed that workers treated with com-
pound B had reduced quantities of normal and branched alkanes
and a lower survival than control workers under water-limited
conditions. These findings are interesting because *int* and its
receptor are both up-regulated when workers age and switch
task from nursing to foraging. Since workers are more likely to
encounter drier environments when they forage, this suggests that
inotocin signalling may be implicated in regulating physiological
adaptations via increased CHC synthesis when workers initiate
foraging.

Our study provides the first evidence that the inotocin sig-
nalling pathway regulates CHC synthesis via *CYP4G1* expression
in insects, and this pathway is up-regulated with age and task
preference in ants. Interestingly, genomic studies revealed that
the inotocin signalling pathway has been lost in the honeybee and
some other species of aphids and flies (16). As these species have
the *CYP4G* gene (45) and expresses CHCs on their body surface,
it is possible that other signalling pathways have taken over the
functions of inotocin signalling in these species, as discussed
previously (16, 22). It will therefore be of interest to compare
the mechanisms of regulation of *CYP4G* gene and CHCs in
these species that have lost the inotocin signalling pathway. Such
comparative studies may also shed light on the ancestral role of
the oxytocin/vasopressin family peptide in insects and vertebrates.

1082 Methods

1083 More details are provided in SI Appendix.

1084 Ants

1085 *C. fellah* colonies were initiated from queens collected after a mating
1086 flight in March 2003 and 2007 in Tel Aviv, Israel. The ants were reared in
1087 an incubator (NIPPON MEDICAL & CHEMICAL INSTRUMENTS CO., LTD) under
1088 controlled conditions (12:12 LD, 30°C, 55~60% RH). For all experiments, we

used workers from four queenright colonies that each had one queen and approximately 500 workers. We used only minor workers with a body size <8 mm. To determine their age, we painted every month all newly-enclosed workers with a unique colour code. Young virgin queens, males and workers were collected at the beginning of mating flights in May 2015 and 2016 in Tokyo and Ibaraki, Japan (*C. japonicus*) and March in 2018 in Rehovot, Israel (*C. fellah*). Wingless mated queens of both species were collected on the ground just after the mating flight.

Quantitative RT-PCR

RNA was extracted with Trizol (Invitrogen) from whole body (Fig. 2F-2K), body parts (Fig. 1, 2C, 2D, 4D-4G, 6A, 6E, SI Appendix, Fig. S1, S5, and S7A), or dissected tissues (Fig. 3L and 4A). RNA from queens was sequentially purified with RNA Plus micro Kit (Qiagen). cDNA was synthesised from 200ng total RNA using a PrimeScript RT Reagent Kit with gDNA Eraser (Takara). qRT-PCR was performed with Takara SYBR Premix Ex Taq II (TLI RNaseH Plus) using 7900HT (Applied Biosystems), a LightCycler 480 (Roche) or MX3000P (Agilent). Primers for qRT-PCR are listed in Table S2. All primers had similar PCR amplification efficiency (~2.0). The most stable reference genes and gene normalisation factors were determined by the software geNorm with Biogazelle software (qbase). We used *ef1a* and *rp2* for whole body, head and abdomen analyses, and *gapdh* and *rp2* for the fat body plus oenocyte and digestive tract analyses. The relative expressions of target genes were scaled against average values in each experiment with the Biogazelle software (qbase).

Quantification of peptide with LC-MS/MS

The detailed procedure for peptide extraction is shown in SI Appendix. The amount of inotocin peptide was quantified by ultra-performance liquid chromatography (ACQUITY System, Waters), equipped with a tandem mass spectrometer, TQD (Waters). Separation was achieved on an AccQ-Tag Ultra RP Column (2.1×100mm, 1.7µm particles, Waters) at 40°C. The two mobile phases consisted of (A) 20mM formic acid and (B) acetonitrile. Linear gradients from 99.9% (A) to 50% (A) were used for the separation at a flow rate of 0.3 ml/min. The effluent was then introduced into TQD, ionised by electrospray ionization with positive ion mode (ESI+), and detected by multiple reaction monitoring (MRM) using the transition of m/z 328.4 to m/z 86.38. Sample concentrations were calculated from the standard curve obtained from serial dilution of synthesised inotocin peptide (Biogate Co., Ltd).

DNA constructs

The cDNA of the *int* and *intR* was obtained by reverse transcription using Prime script™ RT Reagent Kit with gDNA eraser (Takara) and RNA isolated from whole body of *C. fellah* and *C. japonicus* worker from laboratory colony. The oxytocin receptor (OXTR) and *Ga15* were amplified from the following vectors respectively: Human OXTR in pcDNA3.1+ (cDNA Resource Center #OXTR00000), Human *Ga15* in pcDNA3.1+ (cDNA Resource Center #GNA1500000). Detailed procedure to construct *pPB-intR-mcherry* and *pPB-OXTR-mcherry* is shown in SI Appendix.

Generation of antibodies

Polyclonal rabbit antibody to inotocin proprotein was generated with a synthetic peptide CKISDVADREITDLYMVLGNEVSNEILP corresponding to the C terminus of inotocin proprotein (MBL Co., Ltd). Polyclonal rabbit antibody to CYP4G1 was generated with a synthetic peptide RDDLDDIDDRGKRRLLA corresponding from 301 to 319 amino acid sequence of CYP4G1 (Hokudo Co., Ltd). The antibodies were used for immunostaining (Fig. 3D-3J, 4C, and SI Appendix, Fig. S4D) and western blot (Fig. 4B, SI Appendix, Fig. S4B and S4C).

Western blot analysis

We subjected tissue lysates to 12.5% SDS-PAGE analysis and immunoblotting. Rabbit polyclonal antibody to inotocin (1:50), rabbit polyclonal antibody to CYP4G1 (1:500), anti-HistoneH3 antibody (1:500, Cell signaling), anti-myc (1:1000, Invitrogen), anti-βtubulin (1:2000, Invitrogen), anti-gapdh (1:2000, Cell signaling) were used as primary antibodies, whereas horseradish peroxidase-conjugated antibody to rabbit (1:1000, Cell Signaling), antibody to mouse (1:1000, Promega) were used as secondary antibodies. Immobilon Western (Millipore) were used for detection. As negative control, we mixed in a ratio of 1:20 (mol) the antibodies for inotocin and CYP4G1 with their synthesised antigen peptides incubated at 4°C overnight. After the overnight incubation they were stored in 50% glycerol at -20°C. Images were captured with the LAS4000 (GE Healthcare ImageQuant) or Chemidoc™ XRS+ systems (BIO-RAD).

Immunohistochemistry

Whole brain immunohistochemistry was performed as described (66) with some modifications in SI Appendix. Fluorescent images were captured with TCS-SP5 laser scanning confocal microscopy (Leica) with a HC PL Fluotar 10x/0.30 objective (Leica, 506505) or HC PL APO 20x/0.70 objective (Leica, 506513) and the Application Suite Advanced Fluorescence software (Leica) or LSM700 laser scanning confocal microscopy (Carl Zeiss) with a Plan-APOCHROMAT 10X/0.45 or 20X/0.8 objective (Carl Zeiss) and ZEN 2011 software.

in situ hybridisation

To examine *int* mRNA expression in the brain, fluorescent *in situ* hybridisation was performed using RNAscope® Multiplex Fluorescent Reagent Kit 2.0 according to the manufacturer's instructions (Advanced Cell Diagnostics). Detailed protocol is shown in SI Appendix.

dsRNA generation and treatment

Gene-specific 520bp sequences for *intR* (1-520bp) and control *EGFP* (104-623bp) with T7 RNA polymerase sequence at both ends were amplified by PCR with primers listed in Table S3, and *in vitro* transcription was performed using T7 RiboMAX Express RNAi System (Promega) according to the manufacturer's protocol. The concentration and the size of dsRNA were determined with a nanodrop spectrophotometer and electrophoresis. dsRNA was adjusted to 4µg/µl with 300mM sucrose water. The feeding treatments with dsRNA were performed as previously described (51). For first 10 days of the treatment, ants were fed daily with 20µl of dsRNA-sucrose water, then with 20µl sucrose water with no dsRNA during the last 5 days. After these 15 days treatment, RNA was extracted from each body part for qRT-PCR analyses.

Calcium assay and chemical screening

The protocol to generate stable cell lines and cell preparation for calcium assay is shown in SI Appendix. We used Functional Drug Screening System (FDSS7000, Hamamatsu Photonics) to measure the fluorescent level of Fluo-4 with the excitation and emission wavelength bands centered at 480 and 540 nm, respectively. The ligand was diluted with the buffer (20mM HEPES in HBSS) and dispensed to the non-binding 384 well plate (Greiner). 5µl of ligand solution was dispensed to each well with plastic tip (Hamamatsu Photonics) 10 seconds after the measurement started. The fluorescent intensity was measured for 2 min in each plate. The ligands were washed away between each experiment with a cleaning solution (10mM citric acid (Nakarai) in 50% ethanol). The fluorescent intensity from 1 to 10 second, or from 11 to 120 second in the measurement was used in the following formula. Response to the ligand (R) was given by

$$R = \text{Max}(\text{Intensity}_{11-120}) - \text{Average}(\text{Intensity}_{1-10})$$

We performed the chemical screening with 222,400 compounds obtained from the Drug Discovery Initiative (DDI, The University of Tokyo). Detailed procedures for 1st and 2nd chemical screening are shown in SI Appendix.

Binding assay with TR-FRET

Inotocin receptor ligand binding assays were performed using the Tag-lite® assay (cisbio) according to the manufacturer's instructions shown in SI Appendix.

Antagonist injection

To select the appropriate dosage of each compound for injection, we first examined the effect of DMSO on ant survivability, because compound A, B, and C were stocked in DMSO (10mM concentration). We found that 1% of DMSO showed no effect on survivability while 10% of DMSO resulted in high lethality. Therefore, we injected 100µM of compound A (PB03670558, U.O.S.), B (PB153374836, U.O.S.) or C (T5275621, Enamine) in 1% DMSO to avoid negative effects of DMSO. Because atosiban (Sigma-Aldrich) had a weaker inhibition rate (Fig. 5B) than compound A, B or C (Fig. 5H) *in vitro* and because it is soluble in water we used higher concentrations (1mM and 2mM). Ants were anaesthetised on ice and injected into the abdomen through the intersegmental membrane with 1.5 µl of the different compound solution with a IM-300 microinjector (Narishige). Control saline was prepared as the mixture of ant saline with the solvent of each chemical compounds (with water for atosiban (1:10 for 1mM, and 1:5 for 2mM), and with DMSO for compound A, B, and C (1:100)). For the expression analysis of *CYP4G1*, RNA was extracted at 24 hours after the injection of each compounds.

Behaviour tracking system and tracking data processing

Behavioural tracking was performed as described previously (47). Ants were tagged with unique matrix codes (1.6mm side length) after immobilisation on ice. Tracking experiments were performed under controlled conditions (12:12 LD, 30 °C, 55~60% RH). The tracking data were post-processed as described previously (47). Parameters for time spent in the food, distance ant moved, and time spent in the nest were obtained as described previously (67).

Cuticular hydrocarbon analyses

The extraction and quantification of CHCs was performed as described previously (68) with some modifications. Detailed protocol is shown in SI Appendix.

Acknowledgments

We thank A. Hefetz, O. Feinerman for collecting queens, Y. Yamaguchi and T. Chihara for supplying plasmids, A. Crespi and D. Mersch for the technical support for the tracking system, and C. Stoffel and C. La Mendola for gene expression analyses. We thank M. Sakurai, Y. Mawatari, and A. Nakamichi for help with animal keeping, gene expression, and immunohistochemistry analyses. We are grateful to H. Watanabe for technical support for the study of neural anatomy, M. Hojo and M. Kanno for help of analyses of cuticular hydrocarbons, and A. LeBoeuf, T. Onaka, T. Kikusui, R. Benton, and T. Tamura for helpful discussions. We thank T. Fukatsu and members of symbiotic evolution and biological functions research group for the technical assistance and advice. This work was funded by the Grant-in-Aid for Scientific Research on Innovative Areas (No. 4501) from the Japan Society for the Promotion of Science, AMED under Grant Number JP18gm6110014, and in part supported by the Platform Project for Supporting Drug Discovery and Life Science Research from AMED under Grant Number JP17am0101086, and the Swiss NSF. The funders had no role in the study design, data

1225
1226
1227
1228
1229
1230
1231
1232
1233
1234
1235
1236
1237
1238
1239
1240
1241
1242
1243
1244
1245
1246
1247
1248
1249
1250
1251
1252
1253
1254
1255
1256
1257
1258
1259
1260
1261
1262
1263
1264
1265
1266
1267
1268
1269
1270
1271
1272
1273
1274
1275
1276
1277
1278
1279
1280
1281
1282
1283
1284
1285
1286
1287
1288
1289
1290
1291
1292

collection and analysis, decision to publish, or preparation of the manuscript. **AUTHOR CONTRIBUTIONS** AK planned and directed this study, performed experiments, and wrote the manuscript with LK. NM, HT, and TO conducted the pharmacological screening and *in vitro* experiment. NM and MM did

1. Feldman R, Weller A, Zagoory-Sharon O, & Levine A (2007) Evidence for a neuroendocrinological foundation of human affiliation: plasma oxytocin levels across pregnancy and the postpartum period predict mother-infant bonding. *Psychol Sci* 18(11):965-970.
2. Kosfeld M, Heinrichs M, Zak PJ, Fischbacher U, & Fehr E (2005) Oxytocin increases trust in humans. *Nature* 435(7042):673-676.
3. Parreiras ESLT, et al. (2017) Functional New World monkey oxytocin forms elicit an altered signaling profile and promotes parental care in rats. *Proc Natl Acad Sci USA* 114(34):9044-9049.
4. Ross HE & Young LJ (2009) Oxytocin and the neural mechanisms regulating social cognition and affiliative behavior. *Front Neuroendocrinol* 30(4):534-547.
5. Ferris CF, Axelson JF, Martin AM, & Roberge LF (1989) Vasopressin immunoreactivity in the anterior hypothalamus is altered during the establishment of dominant/subordinate relationships between hamsters. *Neuroscience* 29(3):675-683.
6. Ferris CF, Pollock J, Albers HE, & Leeman SE (1985) Inhibition of flank-marking behavior in golden hamsters by microinjection of a vasopressin antagonist into the hypothalamus. *Neurosci Lett* 55(2):239-243.
7. Terranova JJ, Ferris CF, & Albers HE (2017) Sex Differences in the Regulation of Offensive Aggression and Dominance by Arginine-Vasopressin. *Front Endocrinol* 8:308.
8. Winslow JT, Hastings N, Carter CS, Harbaugh CR, & Insel TR (1993) A role for central vasopressin in pair bonding in monogamous prairie voles. *Nature* 365(6446):545-548.
9. Martos-Sitcha JA, Campinho MA, Mancera JM, Martínez-Rodríguez G, & Fuentes J (2015) Vasotocin and isotocin regulate aquaporin 1 function in the sea bream. *J Exp Biol* 218(Pt 5):684-693.
10. Hasegawa T, Tani H, Suzuki M, & Tanaka S (2003) Regulation of water absorption in the frog skins by two vasotocin-dependent water-channel aquaporins, AQP-h2 and AQP-h3. *Endocrinology* 144(9):4087-4096.
11. Goodson JL, Schrock SE, Klatt JD, Kabelik D, & Kingsbury MA (2009) Mesotocin and nonapeptide receptors promote estrilidid flocking behavior. *Science* 325(5942):862-866.
12. Klatt JD & Goodson JL (2013) Oxytocin-like receptors mediate pair bonding in a socially monogamous songbird. *Proc Biol Sci* 280(1750):20122396.
13. Oldfield RG & Hofmann HA (2011) Neuropeptide regulation of social behavior in a monogamous cichlid fish. *Physiol Behav* 102(3-4):296-303.
14. Pedersen A & Tomaszycski ML (2012) Oxytocin antagonist treatments alter the formation of pair relationships in zebra finches of both sexes. *Horm Behav* 62(2):113-119.
15. Yokoi S, et al. (2015) An essential role of the arginine vasotocin system in mate-guarding behaviors in triadic relationships of medaka fish (*Oryzias latipes*). *PLoS Genet* 11(2):e1005009.
16. Liutkeviciute Z, Koehbach J, Eder T, Gil-Mansilla E, & Gruber CW (2016) Global map of oxytocin/vasopressin-like neuropeptide signalling in insects. *Sci Rep* 6:39177.
17. Douzery EJ, Snell EA, Bapteste E, Delsuc F, & Philippe H (2004) The timing of eukaryotic evolution: does a relaxed molecular clock reconcile proteins and fossils? *Proc Natl Acad Sci USA* 101(43):15386-15391.
18. Aikins MJ, et al. (2008) Vasopressin-like peptide and its receptor function in an indirect diuretic signaling pathway in the red flour beetle. *Insect Biochem Mol Biol* 38(7):740-748.
19. Cherasse S & Aron S (2017) Measuring insectin receptor gene expression in chronological order in ant queens. *Horm Behav* 96:116-121.
20. Gruber CW & Muttenthaler M (2012) Discovery of defense- and neuropeptides in social ants by genome-mining. *PLoS One* 7(3):e32559.
21. Liutkeviciute Z, et al. (2018) Oxytocin-like signaling in ants influences metabolic gene expression and locomotor activity. *FASEB J*:fj201800443.
22. Stafflinger E, et al. (2008) Cloning and identification of an oxytocin/vasopressin-like receptor and its ligand from insects. *Proc Natl Acad Sci USA* 105(9):3262-3267.
23. Donaldson ZR & Young LJ (2008) Oxytocin, vasopressin, and the neurogenetics of sociality. *Science* 322(5903):900-904.
24. Insel TR (2010) The challenge of translation in social neuroscience: a review of oxytocin, vasopressin, and affiliative behavior. *Neuron* 65(6):768-779.
25. Neumann ID & Landgraf R (2012) Balance of brain oxytocin and vasopressin: implications for anxiety, depression, and social behaviors. *Trends Neurosci* 35(11):649-659.
26. Wilson E & Hölldobler B (1990) *The Ants* (Springer, Berlin).
27. Smith CR, Toth AL, Suarez AV, & Robinson GE (2008) Genetic and genomic analyses of the division of labour in insect societies. *Nat Rev Genet* 9(10):735-748.
28. Robinson EJ, Feinerman O, & Franks NR (2009) Flexible task allocation and the organization of work in ants. *Proc Biol Sci* 276(1677):4373-4380.
29. Bourke AFG & Franks NR (1995) *Social Evolution in Ants* (Princeton Univ. Press, Princeton, NJ).
30. Huang ZY & Robinson GE (1992) Honeybee colony integration: worker-worker interactions mediate hormonally regulated plasticity in division of labor. *Proc Natl Acad Sci USA* 89(24):11726-11729.
31. Robinson GE, Page RE, Jr., Strambi C, & Strambi A (1989) Hormonal and genetic control of behavioral integration in honey bee colonies. *Science* 246(4926):109-112.
32. Traniello MASaJFA (2006) Age-related repertoire expansion and division of labor in *Pheidole dentata* (Hymenoptera: Formicidae): a new perspective on temporal polyethism and behavioral plasticity in ants. *Behav Ecol Sociobiol* 60:631-644.
33. Gibbs AG, Chippindale AK, & Rose MR (1997) Physiological mechanisms of evolved desiccation resistance in *Drosophila melanogaster*. *J Exp Biol* 200(Pt 12):1821-1832.
34. Gibbs AG (1998) Water-proofing properties of cuticular lipids. *Am Zool* 38:471-482.
35. Wigglesworth V (1945) Transpiration through the cuticle of insects. *J Exp Biol Lond* 21(97-

the LC-MS/MS experiments. SM conducted behavioural experiments and conducted the statistical analyses. MM and LK contributed to the planning of the study. All authors contributed to editing the manuscript. **DECLARATION OF INTERESTS** The authors declare no conflict of interest.

- 114).
36. Chung H & Carroll SB (2015) Wax, sex and the origin of species: Dual roles of insect cuticular hydrocarbons in adaptation and mating. *Bioessays* 37(7):822-830.
37. Boulay R, Hefetz A, Soroker VV, & Lenoir A (2000) *Camponotus fellah* colony integration: worker individuality necessitates frequent hydrocarbon exchanges. *Anim Behav* 59(6):1127-1133.
38. Ozaki M, et al. (2005) Ant nestmate and non-nestmate discrimination by a chemosensory sensillum. *Science* 309(5732):311-314.
39. VanderMeer RK, Breed MD, Espelie KE, & Winston ML (1998) *Pheromone communication in social insects* (Westview Press).
40. Wagner D, et al. (1998) Task-Related Differences in the Cuticular Hydrocarbon Composition of Harvester Ants, *Pogonomyrmex barbatus*. *J Chem Ecol* 24(12):2021-2037.
41. Wagner D, Tissot M, & Gordon D (2001) Task-related environment alters the cuticular hydrocarbon composition of harvester ants. *J Chem Ecol* 27(9):1805-1819.
42. Martin SJ & Drijfhout FP (2009) Nestmate and task cues are influenced and encoded differently within ant cuticular hydrocarbon profiles. *J Chem Ecol* 35(3):368-374.
43. Sturgis SJ, Greene MJ, & Gordon DM (2011) Hydrocarbons on harvester ant (*Pogonomyrmex barbatus*) middens guide foragers to the nest. *J Chem Ecol* 37(5):514-524.
44. Fan Y, Zurek L, Dykstra MJ, & Schal C (2003) Hydrocarbon synthesis by enzymatically dissociated oenocytes of the abdominal integument of the German Cockroach, *Blattella germanica*. *Naturwissenschaften* 90(3):121-126.
45. Qiu Y, et al. (2012) An insect-specific P450 oxidative decarbonylase for cuticular hydrocarbon biosynthesis. *Proc Natl Acad Sci USA* 109(37):14858-14863.
46. Yu Z, et al. (2016) *LmCYP4G102*: An oenocyte-specific cytochrome P450 gene required for cuticular waterproofing in the migratory locust, *Locusta migratoria*. *Sci Rep* 6:29980.
47. Mersch DP, Crespi A, & Keller L (2013) Tracking individuals shows spatial fidelity is a key regulator of ant social organization. *Science* 340(6136):1090-1093.
48. Bloch G, Solomon SM, Robinson GE, & Fahrbach SE (2003) Patterns of PERIOD and pigment-dispersing hormone immunoreactivity in the brain of the European honeybee (*Apis mellifera*): age- and time-related plasticity. *J Comp Neurol* 464(3):269-284.
49. Arrese EL & Soulagues JL (2010) Insect fat body: energy, metabolism, and regulation. *Annu Rev Entomol* 55:207-225.
50. Roma GC, Bueno OC, & Camargo-Mathias MI (2010) Morpho-physiological analysis of the insect fat body: a review. *Micron* 41(5):395-401.
51. Ratzka C, Gross R, & Feldhaar H (2013) Gene expression analysis of the endosymbiont-bearing midgut tissue during ontogeny of the carpenter ant *Camponotus floridanus*. *J Insect Physiol* 59(6):611-623.
52. Di Giglio MG, et al. (2017) Development of a human vasopressin V1a-receptor antagonist from an evolutionary-related insect neuropeptide. *Sci Rep* 7:41002.
53. Simhan HN & Caritis SN (2007) Prevention of preterm delivery. *N Engl J Med* 357(5):477-487.
54. Herington JL, et al. (2015) High-Throughput Screening of Myometrial Calcium-Mobilization to Identify Modulators of Uterine Contractility. *PLoS One* 10(11):e0143243.
55. Maggi M, et al. (1994) Antagonists for the human oxytocin receptor: an *in vitro* study. *J Reprod Fertil* 101(2):345-352.
56. Gimpl G, Postina R, Fahrholz F, & Reinheimer T (2005) Binding domains of the oxytocin receptor for the selective oxytocin receptor antagonist buspiran in comparison to the agonists oxytocin and carbetocin. *Eur J Pharmacol* 510(1-2):9-16.
57. Clipperton-Allen AE, et al. (2012) Oxytocin, vasopressin and estrogen receptor gene expression in relation to social recognition in female mice. *Physiol Behav* 105(4):915-924.
58. Steinman MQ, et al. (2015) Hypothalamic vasopressin systems are more sensitive to the long term effects of social defeat in males versus females. *Psychoneuroendocrinology* 51:122-134.
59. Terranova JJ, et al. (2016) Serotonin and arginine-vasopressin mediate sex differences in the regulation of dominance and aggression by the social brain. *Proc Natl Acad Sci USA* 113(46):13233-13238.
60. Lee HJ, Macbeth AH, Pagani JH, & Young WS, 3rd (2009) Oxytocin: the great facilitator of life. *Prog Neurobiol* 88(2):127-151.
61. Nagasawa M, et al. (2015) Social evolution. Oxytocin-gaze positive loop and the coevolution of human-dog bonds. *Science* 348(6232):333-336.
62. Ferveur JF, Cortot J, Rihani K, Cobb M, & Everaerts C (2018) Desiccation resistance: effect of cuticular hydrocarbons and water content in *Drosophila melanogaster* adults. *PeerJ* 6:e4318.
63. Gospić J, et al. (2017) The Neuropeptide Corazonin Controls Social Behavior and Caste Identity in Ants. *Cell* 170(4):748-759.e712.
64. Manning M, et al. (2012) Oxytocin and vasopressin agonists and antagonists as research tools and potential therapeutics. *J Neuroendocrinol* 24(4):609-628.
65. Melin P, Trojnar J, Johansson B, Vilhardt H, & Akerlund M (1986) Synthetic antagonists of the myometrial response to vasopressin and oxytocin. *J Endocrinol* 111(1):125-131.
66. Ott SR (2008) Confocal microscopy in large insect brains: zinc-formaldehyde fixation improves synapsin immunostaining and preservation of morphology in whole-mounts. *J Neurosci Methods* 172(2):220-230.
67. Koto A, Mersch D, Hollis B, & Keller L (2015) Social isolation causes mortality by disrupting energy homeostasis in ants. *Behav Ecol Sociobiol* 69(4):583-591.
68. Hojo MK, et al. (2009) Chemical disguise as particular caste of host ants in the ant inquiline parasite *Niphanda fusca* (Lepidoptera: Lycaenidae). *Proc Biol Sci* 276:551-558.

1293
1294
1295
1296
1297
1298
1299
1300
1301
1302
1303
1304
1305
1306
1307
1308
1309
1310
1311
1312
1313
1314
1315
1316
1317
1318
1319
1320
1321
1322
1323
1324
1325
1326
1327
1328
1329
1330
1331
1332
1333
1334
1335
1336
1337
1338
1339
1340
1341
1342
1343
1344
1345
1346
1347
1348
1349
1350
1351
1352
1353
1354
1355
1356
1357
1358
1359
1360